

UNCLASSIFIED

Defense Technical Information Center  
Compilation Part Notice

ADP012504

TITLE: Ion Coulomb Crystals and Some Applications

DISTRIBUTION: Approved for public release, distribution unlimited

This paper is part of the following report:

TITLE: Non-Neutral Plasma Physics 4. Workshop on Non-Neutral Plasmas  
[2001] Held in San Diego, California on 30 July-2 August 2001

To order the complete compilation report, use: ADA404831

The component part is provided here to allow users access to individually authored sections of proceedings, annals, symposia, etc. However, the component should be considered within the context of the overall compilation report and not as a stand-alone technical report.

The following component part numbers comprise the compilation report:

ADP012489 thru ADP012577

UNCLASSIFIED

# Ion Coulomb Crystals and Some Applications

Michael Drewsen,

Liv Hornekær, Niels Kjærgaard, Kristian Mølhave, Anne-Marie Thommesen, Zelinda Videsen, Anders Mortensen, and Frank Jensen

*Institute of Physics and Astronomy, University of Aarhus,  
Ny Munkegade, Building 520, DK-8000, Aarhus C, Denmark  
E-mail: drewsen@ifa.au.dk*

**Abstract.** In this contribution, we present some of our recent results involving ion Coulomb crystals in linear Paul traps. A few results regarding single component crystals are discussed, but the main focus is on properties of two-component crystals and their applications in the fields of cold molecular physics and quantum optics.

## SINGLE-COMPONENT ION COULOMB CRYSTALS

When trapped ions are cooled below a certain critical temperature (typically about ten milli-Kelvin) they form spatially ordered structures sometimes referred to as ion Coulomb-crystals. Such crystals of various sizes containing single atomic ion species have now for more than ten years been investigated in various types of traps (See, e.g., Ref. [1-6] and references therein). As examples, in Fig. 1 CCD-images of an ion Coulomb crystals for five different trap potentials are shown.

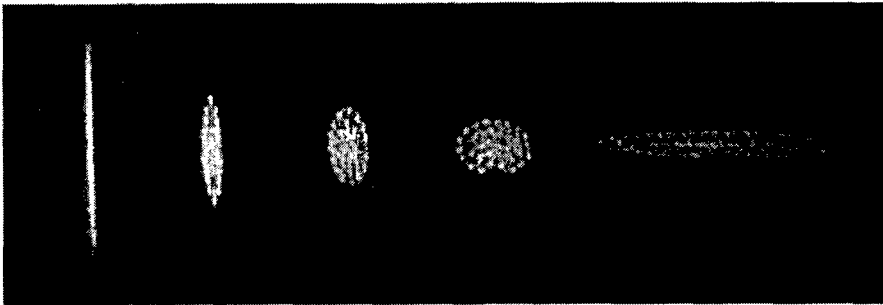


**FIGURE 1.** CCD-images of an ion Coulomb crystal of about  $100\ ^{24}\text{Mg}^+$  ions for five different trapping potentials. The crystals are rotational symmetric around a left-right axis in the figure. The first image corresponds to a nearly pancake-like structure while the last one is cigar-like shaped.

The detailed structures of such crystals have now in a number of experiments been shown to be in good agreement with theoretical predictions [1-6], and the shape of the outer boundary of these cold crystals has been shown to be very similar to that of a cold, homogeneously charged liquid for a large variety of trapping parameters, as seen in Fig. 2 (See also Ref. [7]). Only in extreme limits where the ion Coulomb crystals become one-dimensional string-like or two-dimensional pancake-like, deviations from the liquid model appears. The latter is clearly seen in Fig. 2, when the aspect ratio of the crystal gets above 20.

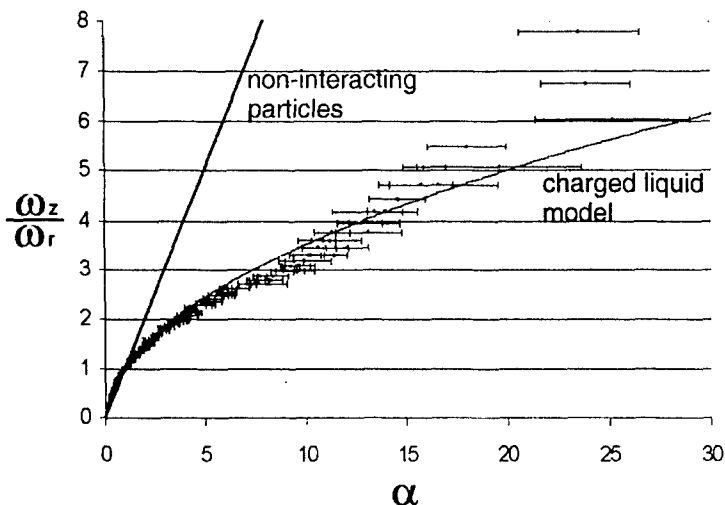


**FIGURE 2.** Measured radial to axial aspect ratio  $\alpha$  of the crystal shown in Fig. 1 for corresponding calculated ratio of the axial to radial trap oscillation frequencies,  $\omega_z/\omega_r$ . The two graphs shows the expected relation between these two quantities in a non-interacting particle and a cold charged liquid model.

So far, only in Penning traps it has been possible to create large enough ion Coulomb crystals that structures associated with infinite two- and three-dimensional crystals (e.g., hexagonal and bcc-structures) have been observed [3,4]. Recently, we have conducted several experiments with large pure ion plasmas created by resonantly enhanced photo-ionization [8] in order to observe similar structures in a linear Paul trap. For the largest ion plasma ( $\sim 15,000$  ions) that can be viewed by the CCD-camera system, we observe no central structures, but only few shell structures at the outer plasma boundary as reproduced in Fig. 3. RF-field induced heating might be one reason for the lack central structures. However, since molecular dynamics simulations with up to  $10^5$  ions (see contribution by H. Totsuji, *et al.* in this proceeding) also seems to fail to reproduce central structures when starting from an initial random distribution, the reason might be more subtle.

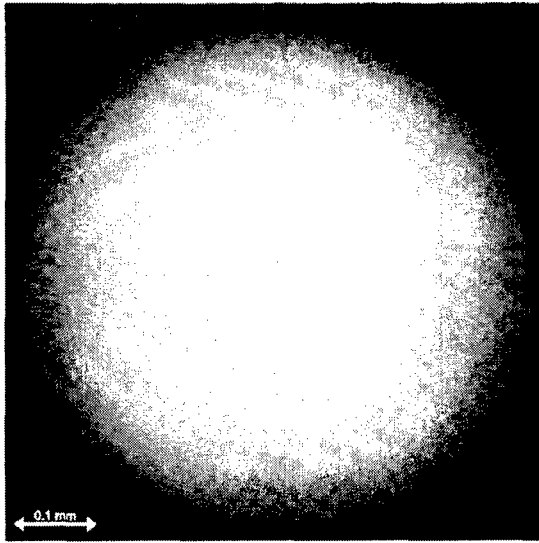


**FIGURE 3.** Cold ion plasma consisting of  $\sim 15,000$   $^{40}\text{Ca}^+$  ions. If fully crystallize, the plasma should consist of about 22 shells, but only a few shells at the outer boundary is observed.

As reported by N. Kjærgaard *et al.* elsewhere in the present proceeding, our group has also recently investigated Coulomb crystals in a pulse-excited Paul trap.

## MULTI-COMPONENT CRYSTALS

Though crystals containing few impurity ions have been observed since the first experiments, so far not much attention has been paid to experimental studies and applications of ion Coulomb-crystals of multi-species. Recently, we have, however, studied some properties of two-component crystals (bicrystals) in linear Paul traps.

### Structures of Two-Species Coulomb Crystals

If more than one ion species is present at the same time in the trap, new more complex orderings appear. In our group we have recently investigated the structures of ion Coulomb crystals containing both laser-cooled  $^{24}\text{Mg}^+$  and  $^{40}\text{Ca}^+$  ions [7]. Examples of pictures of such bicrystals are shown in Fig. 4. The reason for the obvious radial separation of the two ion species is that for singly-charged ions the oscillation frequency along the static field axis of the trap is independent of the ion mass, while in the radial plane the oscillation frequency increases with decreasing mass of the ions. Hence, in the radial plane it is energetically most favorable for the ions to segregate with  $^{24}\text{Mg}^+$  ions closest to the trap axis. The cylindrical structures of the  $^{24}\text{Mg}^+$  ions in these crystals are found to be surprisingly identical to those expected for an infinitely long crystal that is radial confined by a harmonic potential [7]. This similarity is perhaps most obviously seen in Fig. 5, where one observes a string of 47  $^{24}\text{Mg}^+$  ions,

which are equidistantly spaced. Even for crystals with an equal amount of the two ion species, the shape of the outer boundary of the  $^{40}\text{Ca}^+$  part of the crystal is only slightly influenced by the presence of the  $^{24}\text{Mg}^+$  [7].

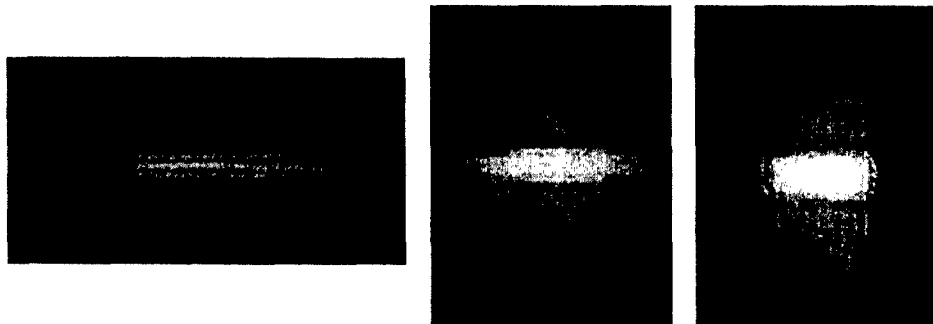


**FIGURE 4.** CCD-images of a bicrystal composed of  $\sim 3000$   $^{40}\text{Ca}^+$  and  $\sim 300$   $^{24}\text{Mg}^+$  ions for three different trapping potentials. The dark gray and the light gray color code correspond to fluorescence from  $\text{Ca}^+$  and  $\text{Mg}^+$  ions, respectively.



**FIGURE 5.** CCD-image of a bicrystal composed of  $\sim 1300$   $^{40}\text{Ca}^+$  and  $47$   $^{24}\text{Mg}^+$  ions (Color code as in Fig. 4). Note that the  $^{24}\text{Mg}^+$  ions are arranged in an equidistant string structure.

We have also initiated investigations of bicrystal structures with other ion species. One interesting example is the case where two ion species with the same charge to mass ratio are present in a linear Paul trap. The result of a molecular dynamics simulation of such a (spherical) bicrystal containing  $150$   $^{40}\text{Ca}^+$  and  $150$   $^{80}\text{A}^{2+}$  ions (here  $^{80}\text{A}$  just means any element or molecule with mass 80) is shown in Fig. 6. Surprisingly, as is immediately observed, the two ion species mixes in common shells. The radius  $R$  of these bicrystals (and hence the shell separation) follows a very simple law:

$$R = (3/(4\pi)(N_{\text{Ca}}/n_{\text{Ca}} + N_{\text{A}}/n_{\text{A}}))^{1/3}, \quad (1)$$

where  $N_{\text{Ca}}$  and  $N_{\text{A}}$  are the numbers of the two ion species, and  $n_{\text{Ca}}$  and  $n_{\text{A}}$  the densities in the case where only the single species is present in the trap.

This law, which essential states that the two species fully mixes, is graphically presented in Fig. 7 together with data obtained from simulations.

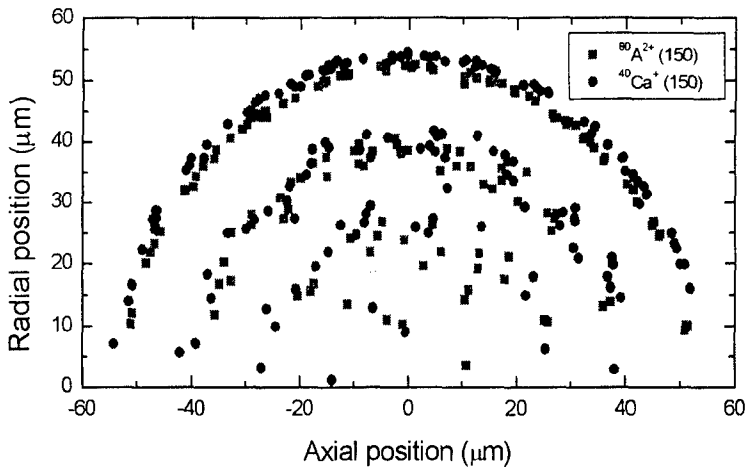


**FIGURE 6.** Results from molecular dynamics simulation of a bicrystal containing 150  $^{40}\text{Ca}^+$  and 150  $^{80}\text{A}^{2+}$  ions in a linear Paul trap. Note how the two ion species mixes in common shells.

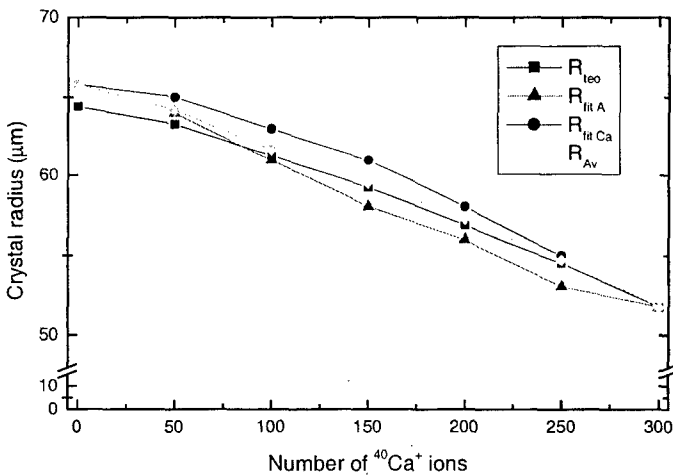


**FIGURE 7.** Radius of spherical bicrystals consisting of  $^{40}\text{Ca}^+$  and  $^{80}\text{A}^{2+}$  ions in a linear Paul trap for various contents of  $^{40}\text{Ca}^+$  ions. The total number of ions is always 300. Notation:  $R_{\text{teo}}$  - radius found from Eq.(1),  $R_{\text{fit A}}$  - radius obtained from fit to position of  $^{80}\text{A}^{2+}$  ions in the outer shell,  $R_{\text{fit Ca}}$  - radius obtained from fit to position of  $^{40}\text{Ca}^+$  ions in the outer shell, and  $R_{\text{Av}}$  - a weighted average of  $R_{\text{fit A}}$  and  $R_{\text{fit Ca}}$ .

## Sympathetic Cooling

One application of bicrystals is to laser cool only one ion species and let the other species be sympathetically cooled through the Coulomb interaction with the directly cooled ions [9-11]. Since the Coulomb interaction is long ranging, one can very effectively achieve sympathetic cooling at time scales of seconds, which is much shorter than the typical storage time (up to hours) of the ions in the trap. An example of the result of sympathetic cooling is shown in Fig. 8. This figure shows the observed fluorescence from laser cooled  $^{40}\text{Ca}^+$  ions (~2000 ions) cooling  $\text{O}_2^+$  molecular ions (~500 ions), formed by electron bombardment of a gas of  $\text{O}_2$  molecules let into the trap vacuum chamber. Since the  $\text{O}_2^+$  ions are lighter than the  $^{40}\text{Ca}^+$  ions, when cooled they form cylindrical structures equivalent to the  $\text{Mg}^+$  ions in Fig. 4, and, indeed, a hollow (non-fluorescing) cylindrical structure is present in Fig. 8. It is generally not easy to obtain a value of the exact temperature of the sympathetically cooled ions, but from pictures like that in Fig. 8, where crystal structures of the laser-cooled  $^{40}\text{Ca}^+$  ions are clearly observed, we can from simulations of such two-component ion plasmas conclude that the temperature cannot be above some tens of milliKelvins. A more direct temperature measurement has been possible with crystals as the ones shown in Fig.4. By observing the fluorescence from  $^{24}\text{Mg}^+$  ions as function of the detuning of a weakly exciting laser an upper temperature can be established from the broadening of the line profile. In Fig. 9, such a profile is presented together with a Voigt-profile fit, which corresponds to a temperature of 45 mK.

Since direct laser cooling can only be applied to a very limited number of singly-charged atomic ions, sympathetic cooling highly expands the possibilities of detailed investigation and manipulation of other ion species including molecular ions, as shown in Fig. 8, and multi-charged ions [12]. The spatial segregation of the ions with different masses makes it, furthermore, possible to, e.g., make a laser beam only interacting with the ion species of interest. For instance, sympathetically cooled ions on a central string in larger bicrystals (see Fig. 5) will be an ideal target for high-resolution spectroscopy and can probably be applied in metrology related research.

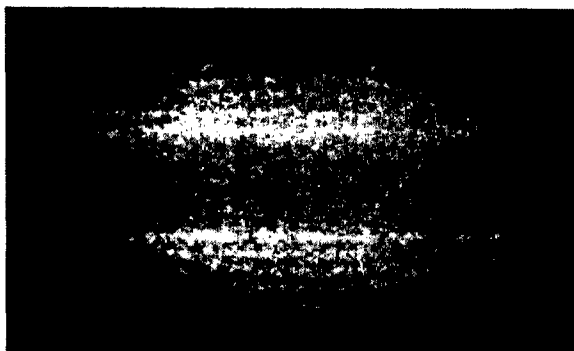


**FIGURE 8.** A bicrystal containing  $\text{O}_2^+$  and  $^{40}\text{Ca}^+$  ions. Since the  $\text{O}_2^+$  ions are lighter than the  $\text{Ca}^+$  ions, they form a cylindrical structure equivalent to the  $\text{Mg}^+$  ions in Fig. 4. This shows up in the picture as a hollow (non-fluorescing) cylindrical structure.

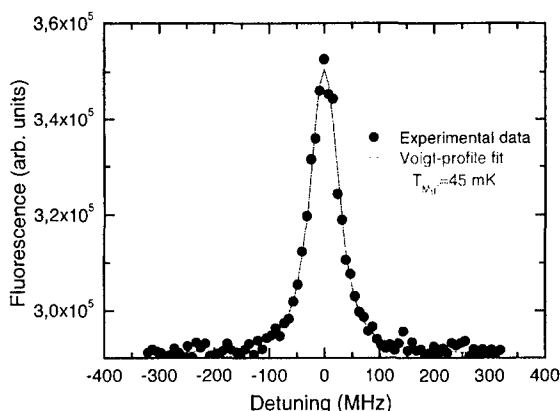


**FIGURE 9.** Fluorescence from  $^{24}\text{Mg}^+$  ions as function of the detuning of a weakly exciting laser. The full circles are the obtained data points, while the full line represents a Voigt-profile fit, which corresponds to a temperature of 45 mK

## COLD MOLECULAR PHYSICS

In the previous section it was shown that molecular ions produced by electron ionization could be trapped and cooled sympathetically to very low translational temperatures. With such a translational cold and spatially localized molecular ion target one can investigate various possibilities of cooling the molecular ion's internal degrees of freedom, i.e., rovibrational motions. From simple theoretical considerations [13], it is not believed that the Coulomb interaction will efficiently cool these degrees of freedom. Due to the multi-level structures of molecules, standard laser cooling will not apply either. However, since the trapping time can be of the order of minutes or more, we plan to investigate various new cooling schemes, which might bring the molecular ions into specific internal states. If this will be achieved, such cold state-specific molecular ions can be an interesting playground for performing, e.g., various coherent-controlled molecular dynamics experiments.

Ion Coulomb crystals are furthermore interesting targets for reaction experiments. So far, we have studied a few reactions between laser-cooled ions in Coulomb crystals and neutral molecules. For larger crystals of  $\text{Mg}^+$  ions we have, e.g., studied photochemical reactions with  $\text{H}_2$  and  $\text{D}_2$  gasses [11]. Monitoring the change in the fluorescence rate from the remaining  $\text{Mg}^+$  ions as a function of reaction time, reaction rates were determined. Furthermore, the reaction product ions could be deduced to be  $\text{MgH}^+$  or  $\text{MgD}^+$  in a non-destructive way by monitoring their radial position with respect to two  $\text{Mg}^+$  isotopes in the Coulomb crystal as illustrated in Fig. 10. By only applying resonant light to the  $^{24}\text{Mg}^+$  ions, isotope specific reactions could be obtained.

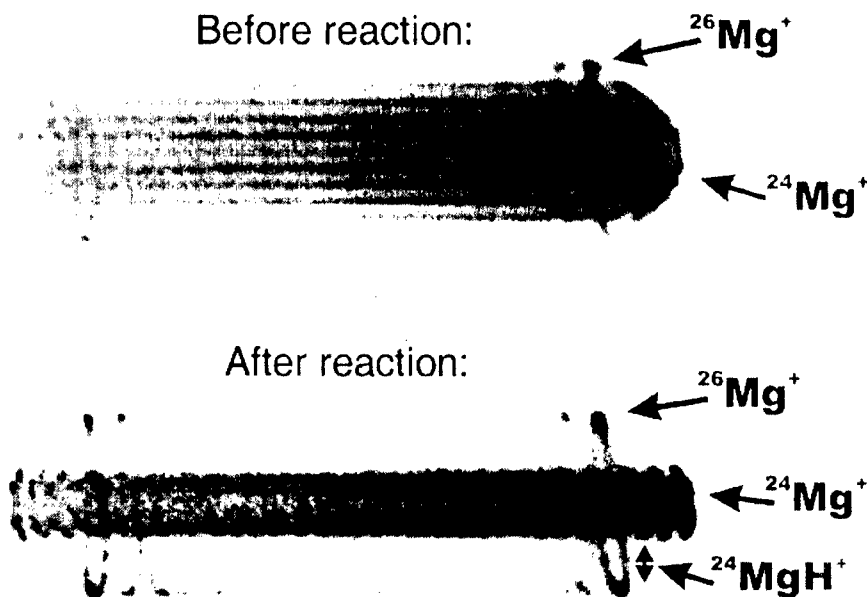


**FIGURE 10.** CCD-images of the fluorescence from  $^{24}\text{Mg}^+$  and  $^{26}\text{Mg}^+$  ions before and after the reaction of  $^{24}\text{Mg}^+$  ions with a  $\text{H}_2$  gas. The product ions  $^{24}\text{MgH}^+$  appear as a non-fluorescent cylindrical region between the two magnesium isotopes.

We have very recently initiated experiments with the aim of studying reaction processes on the single molecule level. This can be achieved by, e.g., initially having a string of laser-cooled  $\text{Ca}^+$  ions, which can individually be monitored by a CCD-camera as shown in Fig. 11a. By introducing a thermal  $\text{O}_2$  gas at a very low pressure (typically  $<10^{-9}$  torr) into the trap region, one can observe how the individual  $\text{Ca}^+$  ions disappear by time and leave non-fluorescing ions in the string, which from additional experiments are known to be  $\text{CaO}^+$  ions (see Fig. 11b). Monitoring the fluorescence integrated over the whole string of ions as a function of time, one observes significant discrete changes in the fluorescence level, revealing the fundamental discrete nature of the reactions. Whether such "digital" information on the reaction processes will give fundamental new insight into chemical reactions is still unclear, but the technique could certainly be used in studies of extremely low rate reactions, due to the long storage time of the cold ions. Since the product ions can typically be trapped and cooled, multi-step reactions can furthermore be studied. An example of the product of a two-step reaction is shown in Fig. 11c. Here the ion string of Fig. 11b has been subjected to a  $\text{CO}$  gas, which in reaction with  $\text{CaO}^+$  leads to reappearance of fluorescing  $\text{Ca}^+$  ions and  $\text{CO}_2$ . A few dark spaces (ions) are still present in Fig. 11c due to unknown impurity reactions.

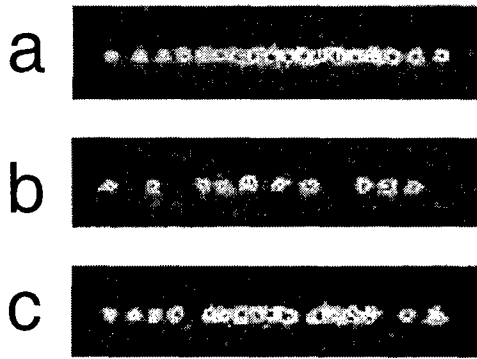


**FIGURE 11.** a) A string of 18 laser-cooled  $\text{Ca}^+$  ions. b) The same string as in figure a), but after reactions with thermal  $\text{O}_2$  molecules, which lead to the production of non-fluorescing  $\text{CaO}^+$  ions. c). The string of ions in Fig. b) after reactions with  $\text{CO}$  molecules. Reactions between  $\text{CaO}^+$  ions and  $\text{CO}$  molecules lead to reappearance of fluorescing  $\text{Ca}^+$  ions and  $\text{CO}_2$ . A few dark spaces (ions) are still present due to unknown impurity reactions.

## QUANTUM MEMORY FOR LIGHT

In order to make future quantum information networks operational, one will need to store quantum information temporarily. Since quantum information most likely will be transferred in the form of light, naturally, one seeks to find appropriate quantum memory devices for quantum states of light.

Recently, two independent experiments have demonstrated that a pulse of coherent light can be temporarily stored as a collective excitation of a cold atomic ensemble [14,15]. The idea behind these experiments suggests that not only coherent light pulses, but also light with non-classical characters can be stored. Both experiments relied on a very large reduction of the group velocity of the light pulse as well as on the atomic medium being optically thick in the absence of a control laser beam. It has, however, been shown that these requirements can be relaxed if the atomic ensemble is placed within a high-finesse optical cavity [16], where the light pulse, due to multiple reflections, will pass the atoms several times. In short, the proposal is based on dynamical impedance matching of the light pulse of interest to an optical cavity with absorption in the form of a stimulated rapid adiabatic transfer process in the atomic media. The absorption rate of the light carrying the quantum information is controlled via a strong classical laser pulse. By the adiabatic transfer process, the initial quantum information of the light pulse is transferred into collective coherent excitation of the atomic ensemble. By a time reversal of the classical light pulse the initial quantum state of light will be regenerated as an output from the cavity.

In our view, the atomic sample in the optical cavity could advantageously be a Coulomb crystal of a few thousand ions. Ions in such crystals may have storage life times of tens of minutes, and have internal state coherence times of the order of a second or more. Using bi-crystals as the ones shown in Fig. 4 and Fig. 8, one species

can be used as the storage medium, while the other can be directly laser cooled and sympathetically cool the “memory” ions.

In such experiments we plan to use  $^{40}\text{Ca}^+$  ions as “memory” ions since they have suitable electronic transitions for the quantum storage of light in the near infrared where non-classical light sources are available. The  $^{40}\text{Ca}^+$  ions will be cooled sympathetically by  $^{44}\text{Ca}^+$  ions, which we plan to load in appropriate amounts using isotope-selective resonant two-photon ionization of an atomic beam [8].

## ACKNOWLEDGMENTS

The presented work has been possible due to financial support from the Danish National Research Foundation, the Danish Research Council, and the Carlsberg Foundation.

## REFERENCES

1. Birkl, G., Kassner, S., and Walther, H., *Nature* **357**, 310 (1992).
2. Drewsen, M., *et al.*, *Phys. Rev. Lett.* **81**, 2878 (1998).
3. Itano, W. M., *et al.*, *Science* **279**, 686 (1998).
4. Mitchell, T. B., *et al.*, *Science* **282**, 1290 (1999).
5. Block, M., Drakoudis, A., Leutner, H., Siebert, P., and Werth, G., *J. Phys. B.* **33**, L375 (2000).
6. Schätz, T., Schramm, U., and Habs, D., *Nature* **412**, 717 (2001).
7. Hornekær, L., *et al.*, *Phys. Rev. Lett.* **86**, 1994 (2001).
8. Kjærgaard, N., *et al.*, *Appl. Phys. B* **71**, 207 (2000).
9. Larson, D. J., *et al.*, *Phys. Rev. Lett.* **57**, 70 (1986).
10. Bowe, P., *et al.*, *Phys. Rev. Lett.* **82**, 2071 (1999).
11. Mølhave, K. and Drewsen, M., *Phys. Rev. A* **62**, 011401(R) (2000).
12. Gruber, L., *et al.*, *Phys. Rev. Lett.* **86**, 636 (2001).
13. Mølmer, K., private communication.
14. Liu, C., *et al.*, *Nature* **409**, 490 (2001).
15. Phillips, D. F., *et al.*, *Phys. Rev. Lett.* **86**, 783 (2001).
16. Lukin, M. D., Yelin, S. F., and Fleischhauer, M., *Phys. Rev. Lett.* **84**, 4232 (2000).